Translational Oncology 13 (2020) 100839

Contents lists available at ScienceDirect

Translational Oncology

journal homepage: www.elsevier.com/locate/tranon

Original research

Tumor-targeted pH-low insertion peptide delivery of theranostic gadolinium nanoparticles for image-guided nanoparticle-enhanced radiation therapy

Wu Liu [a,b,*], John Deacon [c], Huagang Yan [a,d], Bo Sun [a,e], Yanfeng Liu [a], Denise Hegan [a], Qin Li [f], Daniel Coman [g], Maxime Parent [g], Fahmeed Hyder [g,h], Kenneth Roberts [a], Ravinder Nath [a], Olivier Tillement [i], Donald Engelman [c], Peter Glazer [a]

[a] Department of Therapeutic Radiology, Yale University, School of Medicine, New Haven, CT, USA
[b] Department of Radiation Oncology, Stanford University, School of Medicine, Stanford, CA, USA
[c] Department of Molecular Biophysics and Biochemistry, Yale University, New Haven, CT, USA
[d] School of Biomedical Engineering, Capital Medical University, Beijing, China
[e] Department of Radiology, First Affiliated Hospital of Dalian Medical University, Dalian, China
[f] Department of Pulmonary, Critical Care and Sleep, Yale University, School of Medicine, New Haven, CT, USA
[g] Department of Radiology and Biomedical Imaging, Yale University, School of Medicine, New Haven, CT, USA
[h] Department of Biomedical Engineering, Yale University, School of Engineering and Applied Science, New Haven, CT, USA
[i] Univ Lyon Université Claude Bernard Lyon 1, CNRS, Institut Lumière Matière, Lyon, France

ARTICLE INFO

Article history:
Received 24 April 2020
Received in revised form 10 July 2020
Accepted 10 July 2020
Available online xxxx

Keywords:
Metallic nanoparticle radiosensitization
Targeting acidic tumor microenvironment
Cell internalization
Radiation physics
MRI

ABSTRACT

Tumor targeting studies using metallic nanoparticles (NPs) have shown that the enhanced permeability and retention effect may not be sufficient to deliver the amount of intratumoral and intracellular NPs needed for effective *in vivo* radiosensitization. This work describes a pH-Low Insertion Peptide (pHLIP) targeted theranostic agent to enable image-guided NP-enhanced radiotherapy using a clinically feasible amount of injected NPs. Conventional gadolinium (Gd) NPs were conjugated to pHLIPs and evaluated *in vitro* for radiosensitivity and *in vivo* for mouse MRI. Cultured A549 human lung cancer cells were incubated with 0.5 mM of pHLIP-GdNP or conventional GdNP. Mass spectrometry showed 78-fold more cellular Gd uptake with pHLIP-GdNPs, and clonogenic survival assays showed 44% more enhanced radiosensitivity by 5 Gy irradiation with pHLIP-GdNPs at pH 6.2. In contrast to conventional GdNPs, MR imaging of tumor-bearing mice showed pHLIP-GdNPs had a long retention time in the tumor (>9 h), suitable for radiotherapy, and penetrated into the poorly-vascularized tumor core. The Gd-enhanced tumor corresponded with low-pH areas also independently measured by an *in vivo* molecular MRI technique. pHLIPs actively target cell surface acidity from tumor cell metabolism and deliver GdNPs into cells in solid tumors. Intracellular delivery enhances the effect of short-range radiosensitizing photoelectrons and Auger electrons. Because acidity is a general hallmark of tumor cells, the delivery is more general than antibody targeting. Imaging the *in vivo* NP biodistribution and more acidic (often more aggressive) tumors has the potential for quantitative radiotherapy treatment planning and preselecting patients who will likely benefit more from NP radiation enhancement.

Introduction

Despite the increased interest in metallic nanoparticle (NP) radiosensitization for radiation therapy (RT) during the past decade, there has been very limited translation to a clinical setting [1,2]. The major challenges are (i) the specificity of tumor targeting, (ii) the ability to image NP distribution *in vivo* for treatment plan optimization, and (iii) the rapid clearance of conventional NPs *in vivo*. To overcome these challenges and complement the increasing use of MRI for RT planning and on-board imaging, we propose the use of pH-Low Insertion Peptides (pHLIPs) to actively target gadolinium (Gd) NP delivery into cells in tumors.

Under specific conditions, NPs will tend to concentrate within tumors, presumably due to the leaky tumor vasculature and lack of effective lymphatic drainage referred to as the enhanced permeability and retention (EPR) effect [3]. Therefore, NP radiosensitization has become an attractive approach for improving therapeutic ratios in RT. Recent early phase clinical trials [2] of theranostic Gd-based NPs showed a promising potential for

Abbreviations: NP, nanoparticle; pHLIP, pH-Low Insertion Peptide; Gd, gadolinium; RT, radiation therapy; EPR, enhanced permeability and retention; GdNP, gadolinium nanoparticle; PBS, phosphate buffered saline; ICP-MS, inductively coupled plasma mass spectrometry; DCE, dynamic contrast-enhanced.

* Corresponding author at: Department of Radiation Oncology, Stanford University, School of Medicine, 875 Blake Wilbur Dr, MC 5847, Stanford, CA 94305, USA.
E-mail address: wuliu@stanford.edu. (W. Liu).

http://dx.doi.org/10.1016/j.tranon.2020.100839

clinical translation. However, passive targeting based on the EPR effect itself may not be sufficiently specific to tumors, having produced a relatively low tumor-to-normal-tissue uptake ratio, and achieving minimal retention over therapeutic time windows. For example, small gold NPs (*e.g.*, ~2 nm in diameter) are mostly cleared by kidneys within minutes [4], showing effectively zero cellular uptake [5].

Commercially available AGuIX, which is a ~3 nm gadolinium-based NP (GdNP), is an effective contrast agent for MR imaging [6]. Each AGuIX GdNP is composed of a polysiloxane network surrounded by ~10 Gd chelates. The use of GdNPs facilitates NP concentration measurement and tumor diagnosis, and aligns with the emerging trend of MRI-based RT. Measurement of NP concentration in tumor and normal tissue is important for clinical translation as they are needed for quantitative RT treatment planning that takes into account NP radiosensitization and for the determination of optimal irradiation timing. The ultra-small size of AGuIX GdNPs should reduce internal absorption of Auger electrons within the NPs, leaving them free to contribute to antitumor activity; and might allow infiltration through the nuclear pore to further increase proximity to their site of action and thereby potential effectiveness [7,8]. Studies [9] indicated 10–150% enhanced cell killing *in vitro* for various cell types and for both kV and MV X-rays using AGuIX at concentrations of ~1–200 mg Gd/kg.

Although photoelectrons may have a range of nearly 10 μm (on the order of the diameter of a somatic cell), the absorbed dose from Auger cascade electrons generated in GdNPs typically falls off to <1% within 1 μm [9]. Theoretical calculations showed that radiosensitization critically depends on accurate tumor-targeted delivery and furthermore the delivery of NPs inside the tumor cell and close to their nuclear DNA target and other vital structures, such as mitochondria. Monte Carlo simulations predicted that the enhancement of a DNA double strand break would be marginal if the NPs were placed a few μm away from the DNA [10]. This has also been demonstrated *in vitro* [11], where significantly improved radiation dose enhancement was achieved when the cells were allowed to endocytose AGuIX in contrast to extracellular NPs. Since the pHLIP-NP conjugate can deliver cargoes the size of NPs into the cytoplasm, as is the case for large molecules of Peptide Nucleic Acids [12], cytoplasmic delivery should enhance therapeutic efficacy. Our proof-of-concept work demonstrates that use of the pHLIP-NP construct enables both radiation sensitization effectiveness in cell culture and tumor imaging with mouse MRI *in vivo*.

A serious limitation for most cancer diagnostic and therapeutic agents is their lack of tumor-specific distribution or activity. Thus active targeting, as in the use of NPs conjugated to an antibody to target a tumor-specific antigen, is now a major research interest [13,14]. However, recent studies have raised questions about the efficacy of this approach because of limited penetrance and resistance due to tumor heterogeneity. Targeting therapy to a genetically controlled marker has the pitfall of selecting for resistant cells that survive from within heterogeneous tumors, frequently leading to drug-resistant recurrence. Also, while targeting NPs to tumors *via* an antibody may achieve some internalization through receptor-mediated endocytosis, the vast majority of antibody-targeted agents remain superficial to the cancer cell. Furthermore, histologic results revealed that antibody conjugated gold NPs mostly stain peripheral tumor regions and do not penetrate deeply into tumors [14].

pHLIPs have been used to selectively target tumors based on a different type of biomarker: acidity, and enable delivery of some large, polar cargoes directly into tumor cells [15]. Tumors become acidic throughout as a result of their rapid growth, supported by augmented glycolytic metabolism (the Warburg effect), the action of carbonic anhydrases, and hypoxia/ischemia secondary to outgrowth of the blood supply. While the pH of healthy tissues is a slightly basic 7.4, tumors commonly produce an acidic extracellular pH of ~6.2–6.9, and the surfaces of tumor cells are substantially more acidic (pH 6.0–6.5) [16]. Unlike expressed tumor biomarkers, which can be evaded leading to resistance as a result of the selective pressure of treatment, acidity is an unavoidable physiological consequence of cancerous growth, is present in virtually all solid tumors including small metastases, and is not shared by healthy cells. Targeting treatment using tumor acidity may therefore avoid some of the limitations of antibody-targeted therapies. Mouse fluorescent imaging has demonstrated pHLIPs can target solid tumors and small metastases of <1 mm in diameter [17] with ramifications in both diagnosis/prognosis and therapy of advanced cancers.

A typical pHLIP is a ~40 amino acid peptide. It binds reversibly to cell membranes at physiological pH 7.4. In acidic environments, however, it spontaneously inserts across the membrane as a transmembrane α-helix and can translocate moderately large and polar cargoes attached to its inserting C-terminus into the cytosolic compartment of targeted cells. It should therefore be possible to deliver radiosensitizing GdNP agents into the cytosolic compartment of cancer cells by conjugating the agents to pHLIP's C-terminus using a disulfide bond. The disulfide bond is an excellent linker for intracellular drug release because the cytosol has ~1000-fold greater reductive potential than the cell exterior, and the reductive potential is ~2-fold stronger in cancer cells than in most healthy cells, creating a conjugate that is relatively stable in the blood but that releases the cargo upon insertion into the cancer cell cytosol. Using pHLIPs to deliver GdNPs in a tumor-specific intracellular fashion could make an effective dose safer or make the maximum safe dose more effective.

Materials and methods

pHLIP-GdNP conjugation

Using the “wild type” sequence of pHLIP, we produced pHLIP-GdNP conjugates from Npys-protected C-terminal-cysteine pHLIPs (pHLIP-Cys) by a disulfide exchange reaction with thiol-bearing AGuIX GdNPs in organic solvent (chemical diagram Fig. 1).

The AGuIX NPs do not present a thiol group on the surface. To introduce a thiol group on the AGuIX, Traut's reagent (a cyclic imido ester) was incubated with AGuIX for 1 h at room temperature and at pH 8 to react with the amino group on the surface of NPs as described in [18]. Thiol quantification using Ellman's reagent indicates around 1 thiol per AGuIX-SH NP [18]. The mean hydrodynamic diameter of AGuIX-SH NPs is 4.7 nm and the zeta potential is −41 mV at pH 7.4.

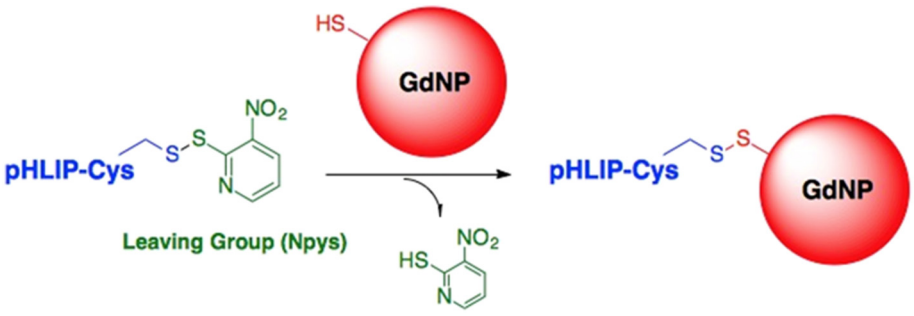

Fig. 1. pHLIP-GdNP conjugation. A disulfide exchange reaction was used to produce pHLIP conjugates with unfunctionalized AGuIX GdNPs. Each GdNP is composed of a polysiloxane network surrounded by ~10 Gd chelates.

We combined between 1.2 and 2.0 molar equivalents pHLIP-Cys(Npys) (molecular weight ~4400 Da) with 1 equivalent of thiol-bearing GdNPs (average molecular weight ~8500 Da) to saturate all thiols on the NPs with pHLIPs. Note that AGuIX-SH is an intermediate compound that should not be present outside the cell on its own, as it is only released from the conjugate upon reduction of the disulfide linker in the cytosol. The reaction was stirred for ~12 h under nitrogen atmosphere at ambient temperature. The product was then washed sequentially with methylene chloride and chloroform, dried under vacuum, resuspended in water, and lyophilized to remove residual solvent. The conjugates were then used in our *in vitro* and *in vivo* experiments.

Unlike other intracellular delivery systems, such as cell penetrating peptides, pHLIPs specifically target the acidity of tumors, and are nontoxic [15]. Neither AGuIX [19,20] nor pHLIP [21] has shown toxicity in animals even at high doses. In addition, the AGuIX-SH + peptide approach has been shown to be safe *in vitro* and *in vivo* for two peptides [18]. We therefore do not expect toxicity of pHLIP-GdNP. Full toxicity tests, however, are warranted for future development.

In vitro radiosensitization assay

We evaluated the radiosensitizing potential of pHLIP-GdNP compared to untargeted commercial AGuIX NPs (without thiol modification), using a pH-dependent clonogenic survival assay. Briefly, cultured authenticated A549 human lung adenocarcinoma cells (purchased from ATCC – the American Type Culture Collection) were treated with NPs at 0.5 mM Gd concentration for 2 h at physiological pH 7.4 or tumoral pH 6.2, then irradiated with 5 Gy of 250 kVp X-ray. To adjust the pH, we slowly added hydrochloric acid to Leibovitz's L-15 medium. The pH of the solution was measured using an Orion Star A111 pH meter. When using this media for treatment (2 h) it is under 0% CO2 at 37 °C. We then removed the media, washed the cells twice with phosphate buffered saline (PBS), trypsinized, spun for 5 min at 1000 $\times g$, aspirated off supernatant, and resuspended the cells in regular media (RPMI with 10% foetal bovine serum (FBS)). The cells were then counted and seeded at 1000 cells per well in 6-well plates. After growing for 8–10 days, the cells were stained with 1% crystal violet, 10% ethanol dye solution. After drying, the plates were digitally scanned and the colonies were manually counted to characterize the viability/survival of the cells after treatment. These experiments were repeated three times.

Measurement of in vitro cellular uptake

Quantified overall bulk cellular uptake was measured by inductively coupled plasma mass spectrometry (ICP-MS), which is capable of detecting very low concentrations of metals. Cultured A549 cells were incubated for 2 h at pH 6.2 with AGuIX and pHLIP-GdNPs at 0.5 mM Gd concentration respectively. This concentration is close to the reported most efficient incubation concentration of AGuIX for cell internalization [22]. Even though the AGuIX tested in [22] has Gd chelated at the surface based on DTPA (not on DOTA), the main ideas remain similar and similar concentration behavior was observed. After washing away excess/extracellular NPs with PBS, ICP-MS analysis was performed on experimental and control fractionated cell samples for each condition to measure the Gd concentration (ELAN DRC-e, SCIEX PerkinElmer).

Mass cytometry by time-of-flight combines flow cytometry and mass spectrometry, providing simultaneous measurement of a large number of cellular parameters at single cell resolution [23]. We used mass cytometry to detect the Gd content at the single cell level. Cultured A549 cells were incubated for 2 h at pH 6.2 with AGuIX at 0.5 mM Gd and pHLIP-GdNP at 0.02 mM Gd concentration, respectively. A lower Gd concentration for pHLIP-GdNP was used because the higher incubation concentration necessary for AGuIX saturated the mass cytometry device (CyTOF2, Fluidigm). After incubation, the cells were washed twice with PBS at pH 7.4 to remove excess/extracellular NPs, then fixed in the presence of an iridium-based Ir-191/193 DNA intercalator at room temperature for 1 h. The DNA-intercalator is used to enable the CyTOF to differentiate nucleated cells from debris based on the mass of the elements.

In vivo mouse tumor MRI

To prepare for MR imaging, 2×10^5 authenticated EMT6 mouse mammary cancer cells were injected to establish tumors in 6-week old female BALB/c mice (EMT6 cells are syngeneic with the BALB/c strain). The animal study was approved by Yale University IACUC (Institutional Animal Care and Use Committee) under protocol 2016-07902. Tumor volume was measured by external Vernier calipers (calculated using the formula for a hemiellipsoid $V = 1/2(4\pi/3)(L/2)(W/2)(H) = 0.5236$ LWH). When tumors reached 100 mm^3, the mice were scanned using an 11.7 T Bruker MR spectrometer under mildly inhaled isoflurane anesthesia (0.5%) in oxygen. Three mice were imaged in this pilot study to investigate the feasibility of MR imaging. The animal experiments comply with the National Institutes of Health guide for the care and use of Laboratory animals (NIH Publications No. 8023, revised 1978).

Mouse #1

Dynamic contrast-enhanced (DCE) MRI scans were performed during tail vein injection of contrast agent to analyze the tumor vasculature and perfusion. DCE acquisition consisted of dynamic spoiled gradient-echo (TR/TE = 19.5/11.5 ms, $\theta = 15^\circ$, 2 averages, 128 × 128) repeated every 5 s for 22 min. At 2 min, a bolus of 0.25 mmol/kg Gadavist (Bayer AG) was injected and flushed with 100 μl of heparinized saline. A multi-TR acquisition was used before and after the DCE sequence to measure the intrinsic and contrast-enhanced longitudinal relaxation rate R_1 ($=1/T_1$) from a single exponential fit. We also used a new MR spectroscopic imaging method – biosensor imaging of redundant deviation in shifts (BIRDS) [24] – with $TmDOTP^{5-}$ infusion to obtain an *in vivo* extracellular pH map. The BIRDS method is based on detecting non-exchangeable chemical shifts from the $TmDOTP^{5-}$ agent itself. The ^{1}H-spectrum of the $TmDOTP^{5-}$ exhibits paramagnetically-shifted and highly pH sensitive resonances with fast relaxation times, allowing rapid signal averaging for high signal-to-noise ratio.

Mice #2&3

AGuIX or pHLIP-GdNP in sterile PBS were injected parenterally at a dose equivalent to 30 μg Gd per gram of mouse body weight ($=0.2$ mmol/-kg total Gd). The mice were scanned 30 min after the injection to quantify T_1 in the tumor and surrounding tissue (see above). The mouse with pHLIP-GdNP injection was scanned again 9 h after the injection.

Results and discussions

In vitro radiosensitization

Results of the clonogenic survival assays, comparing AGuIX and pHLIP-GdNP at pH 7.4 and pH 6.2 for their ability to sensitize cultured A549 cells to 5 Gy radiation, are shown in Fig. 2. The plots are normalized to the control data (no radiation and without NP treatment to the control cells). There are two key observations supporting our hypothesis that using pHLIP-targeted GdNPs increases uptake in tumor cells: (i) at the same concentration, pHLIP-GdNPs resulted in enhanced radiosensitization compared to AGuIX, which can be explained by the differences in cellular uptake and the improved effectiveness when the GdNPs are inside the cells; (ii) more importantly, at the same pHLIP-GdNP concentration, 5 Gy radiation killed more cells at pH 6.2 than at pH 7.4, which implies that pHLIPs targeted the acidic microenvironment and delivered GdNPs into tumor cells, since the pHLIP would not be expected to reduce the surface binding at pH 7.4. Note that the pHLIP-GdNP has a small effect at pH 7.4 compared to AGuIX (Fig. 2). One possible explanation is that pHLIPs tend to bind to the cell membrane so that their linked GdNPs are relatively closer to the cells rather than floating in the media. Nevertheless, the comparison of 5 Gy + pHLIP-GdNP at pH 6.2 *vs* pH 7.4 provides strong evidence for the

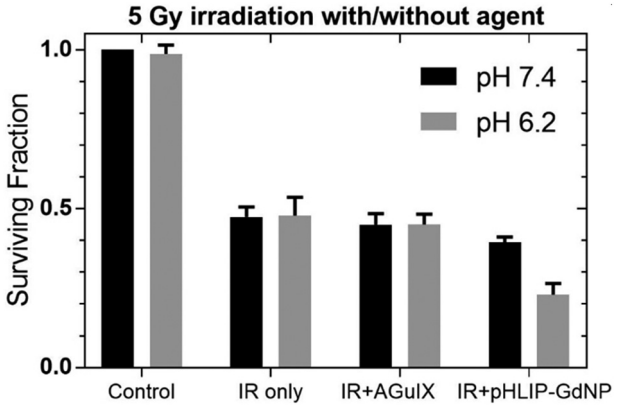

Fig. 2. *In vitro* radiosensitization. Cell survival after 5 Gy X-ray irradiation following treatment with AGuIX or pHLIP-GdNP at pH 7.4 (black) or pH 6.2 (gray), *vs.* untreated and irradiation only controls. Data are normalized as a fraction of pH 7.4 sham treated non-irradiated control cells.

effectiveness of pHLIP-GdNP's acidity targeting and cell internalization, motivating further exploration and development.

In vitro cellular uptake

Results of ICP-MS analysis of the soluble fraction of lysed cells, previously treated in culture with AGuIX or pHLIP-GdNP at pH 6.2, show that on average, the Gd concentration of pHLIP-GdNP incubated cells is 78-fold higher than that of AGuIX incubated cells (Fig. 3a). If we assume 1200 um^3 A549 cell volume [25], then the Gd concentration in AGuIX incubated cells is on average 0.23 mM Gd (comparable to that shown in [26]), while an 18.2 mM Gd concentration is achieved in pHLIP-GdNP incubated cells. While treated cells were washed multiple times prior to fractionation, it is still possible that some small amount of membrane bound, uninserted pHLIP-GdNP may be present; however, this portion is likely to partition with the insoluble fraction.

Histograms of Gd and Ir signal intensity from CyTOF analysis, after gating off the signal from the debris are shown in Fig. 3b. The Ir content is similar for control, AGuIX, and pHLIP-GdNP, indicating similar uptake of the intercalator by DNA. The Gd "signal" intensity is extremely low for the control (pure noise). Different Gd uptakes are evident for both AGuIX and pHLIP-GdNP incubated cells. The concentration in different cells can be different by 2 orders of magnitude. Although the incubation media concentration for pHLIP-GdNP is 25-fold less than that for AGuIX, the cellular uptake is still on average 3.3-fold higher, consistent with the ICP-MS results above.

In vivo mouse tumor MRI

Mouse #1

The DCE-MRI images (Fig. 4) show that the tumor periphery is well vascularized, but the core is not. The *in vivo* extracellular pH map of the same tumor (Fig. 5) confirms the tumor's acidic microenvironment (pH ~6.9) compared to the surrounding normal tissue (pH ~7.3). The degree of tumor acidity has been shown to correlate with aggressiveness [27,28]. Therefore, pHLIP-GdNP may be useful as a prognostic indicator since fluorescent-tagged pHLIPs have been shown to stain tumors of lower pH with greater intensity than tumors of less acidic pH [17]. This may have relevance in selecting patients who will likely benefit more from NP radiation enhancement. The *in vivo* NP distribution may potentially provide a means for quantitative treatment planning to take into account the NP enhancement. Herein, pH measurement with MR (BIRDS) is used to validate the idea that pHLIP-GdNP specifically labels acidic tissues.

Mice #2&3

At 30 min after injection of 0.2 mmol Gd/kg, for both AGuIX and pHLIP-GdNP, the T_1 contrast is high at the tumor periphery, but not substantial in the core region (Fig. 6). At 9 h after injection, the tumor core is also substantially enhanced (*i.e.*, lower T_1) by pHLIP-GdNP. This demonstrates the long retention in tumor and good penetration for pHLIP-GdNP, suitable for the RT workflow, in particular, hypofractionation. The effect of the Gd contrast on relative T_1 enhancement is expected to be even greater at lower magnetic field. *In vivo* studies [9] demonstrated AGuIX's radiosensitizing efficacy could be observed at tumor Gd concentration of as low as 1–10 μg Gd/g of body weight. This supports the idea that effective radiation sensitization can be achieved at very low concentrations of pHLIP-GdNP injection (similar to those needed for MR imaging, which is normally ~15–30 μg Gd/g (0.1–0.2 mmol/kg in Gd) of body weight in humans and can be higher in animal studies).

Providing a bolus of glucose by either oral or parenteral route has been shown to enhance tumor acidity by 0.2–0.5 pH units, peaking at around 1 h after administration, while not affecting healthy tissues [29,30]. For future clinical applications, this strategy might be used to increase the pH contrast and enhance pHLIP-GdNP targeting, retention and insertion.

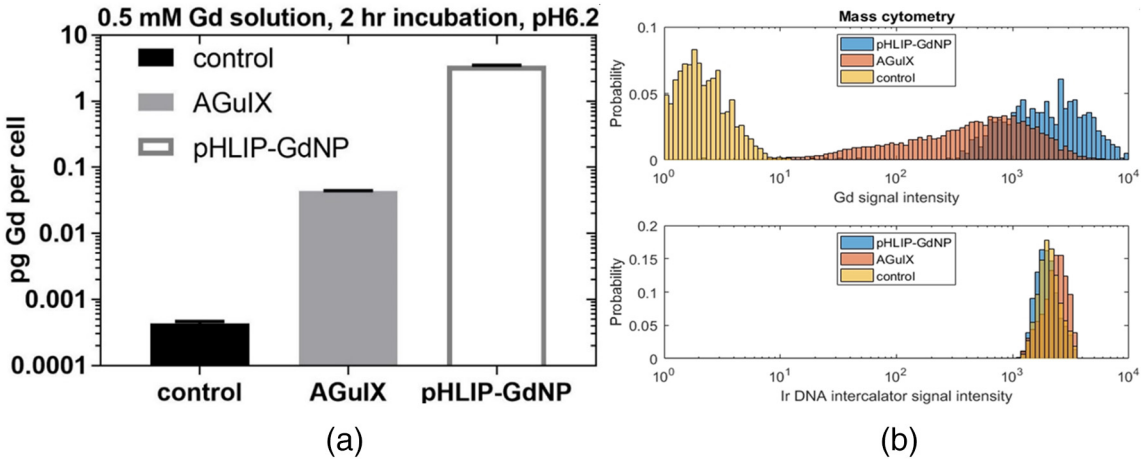

Fig. 3. Cell internalization. (a) ICP-MS analysis of pH 6.2 treatments for Gd concentration in picogram per cell. pHLIP-GdNP treated cells (white) contain 78-fold more intracellular Gd than AGuIX treated cells (gray), after 2 hour incubation at 0.5 mM, *in vitro* (y-axis is in log scale). (b) Mass cytometry measurements of Gd cellular uptake (upper panel) and Ir DNA intercalator uptake (lower panel) at single cell resolution. The incubation concentration for pHLIP-GdNP is 25-fold lower than for AGuIX due to signal saturation at higher concentrations, indicating far more uptake of the pHLIP-conjugated NPs (0.02 mM pHLIP-GdNP, 0.5 mM AGuIX).

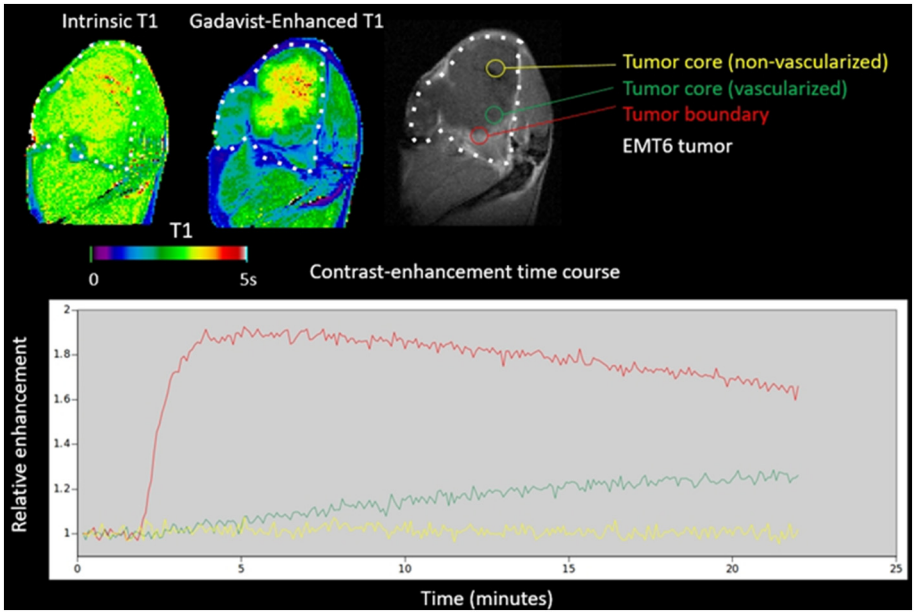

Fig. 4. DCE-MRI of an EMT6 mouse tumor *in vivo*. The tumor periphery (red) is well vascularized, but large volumes of the core (yellow) are not. NPs relying on EPR for tumor targeting typically have poor penetration into such poorly-vascularized regions of the tumor. (For interpretation of the references to colour in this figure legend, the reader is referred to the web version of this article.)

Conclusion

This feasibility study examines GdNPs linked to pHLIP as a novel agent for simultaneously imaging and radiosensitizing solid tumors. Conjugation of pHLIP to GdNPs actively targets a solid tumors' acidic microenvironment and also delivers otherwise cell-impermeable, radiation sensitizing NPs into cancer cells, which is critical for the NP-induced short-range Auger and photoelectrons to effectively reach vital cellular targets. Such targeting and delivery could lead to NP-enhanced RT at a clinically-optimized amount of injected NPs. Magnetic resonance imaging with pHLIP-GdNP can be used to examine NP distributions *in vivo* and to possibly facilitate enhanced quantitative RT treatment planning. Moreover, it is likely that the present construct can be improved, for example by using pHLIPs with different properties [31]. This pilot study initiates the possibility of future development of a clinically relevant treatment planning system, allowing proactive radiation dose calculations based on *in vivo* NP distribution estimated by MRI as well as direct *in vivo* pH mapping. Thus, the method described here represents the important first step in developing and translating a combination of novel, actively-targeted NP radiosensitization and MR imaging for clinical use.

Funding

This project has been supported by a Yale Cancer Center Pilot grant and National Institutes of Health grants R21 EB-026553 (to WL), R01 GM-073857 (to DME), and R01 EB-023366 (to FH). The funding sources were not involved in the study design, data collection and analysis, and manuscript preparation.

Declaration of competing interest

O.T. is the co-founder and CSO of NH Theraguix, but the company did not fund any part of the work reported in the paper. D.M.E is a founder of pHLIP, Inc. and has shares in the company, but the company did not fund or participate in any part of the work reported in the paper. P.M.G is a founder of and consultant for Cybrexa Therapeutics. P.M.G. is a consultant for

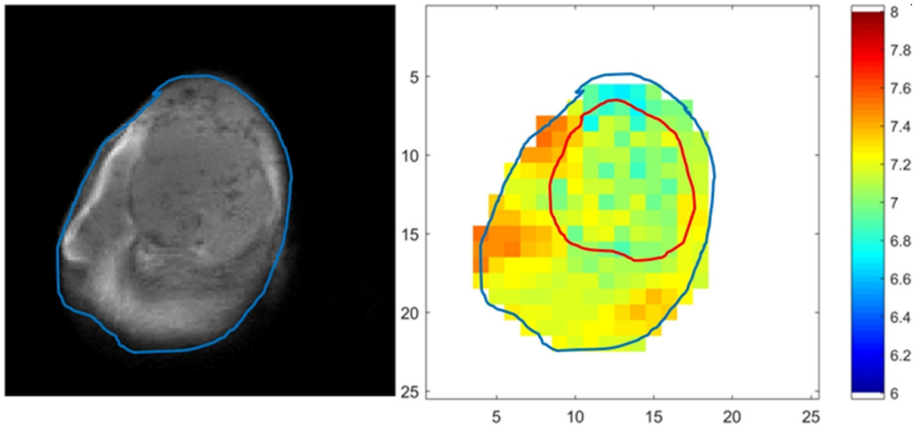

Fig. 5. T_1 weighted MR image and extracellular pH mapping of the EMT-6 mouse tumor *in vivo*. The tumor is clearly visible on the MR image (left), and is marked by the red contour in the pH map (right). The tumor is acidic (bulk extracellular pH ~6.9) compared to surrounding normal tissue (pH ~7.3). (For interpretation of the references to colour in this figure legend, the reader is referred to the web version of this article.)

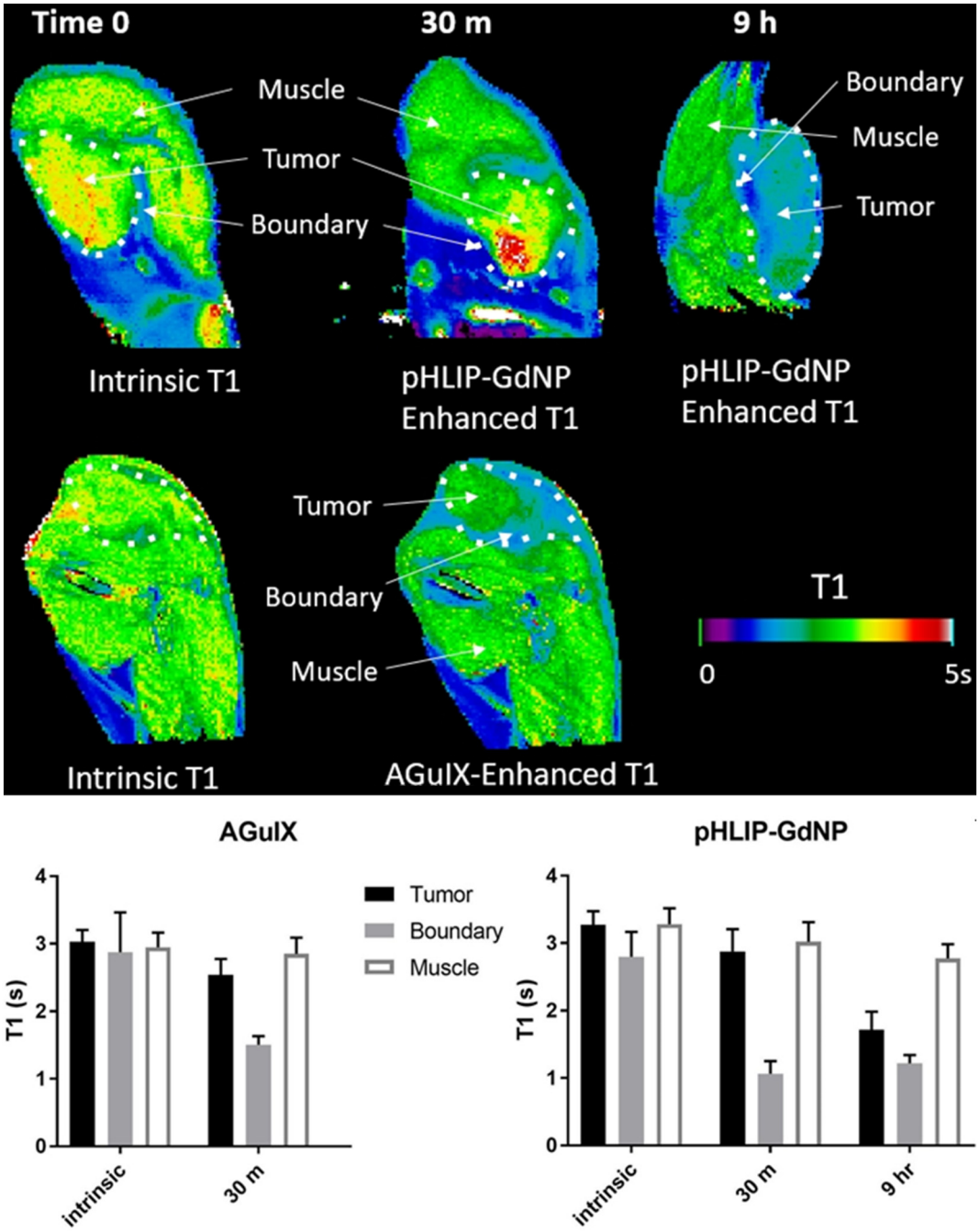

Fig. 6. *In vivo* mouse MRI with injected pHLIP-GdNP or AGuIX. MRI T_1 measurements show tumor *vs* muscle contrast – lower T_1 is higher contrast. The lower panel shows the measured T_1 values.

pHLIP, Inc.. Neither company funded or participated in any part of the work reported in the paper. The other authors declare that they have no known competing financial interests or personal relationships that could have appeared to influence the work reported in this paper.

Acknowledgements

We thank Mr. Paul Bongiorni and Dr. Meetu Kaushik for their helps on radiobiology experiments.

CRediT author contribution statement

Wu Liu: Conceptualization, Methodology, Validation, Formal analysis, Investigation, Resources, Data Curation, Writing - Original Draft, Writing - Review & Editing, Visualization, Supervision, Project administration, Funding acquisition. **John Deacon:** Methodology, Validation, Investigation, Writing - Review & Editing, Visualization. **Huagang Yan:** Validation, Formal analysis, Investigation, Data Curation, Writing - Review & Editing. **Bo Sun:** Investigation. **Yanfeng Liu:** Validation, Investigation, Project administration; **Denise Hegan:** Validation, Investigation, Project administration. **Qin Li:** Formal analysis, Resources. **Daniel Coman:** Software, Formal analysis, Writing - Review & Editing, Visualization.; **Maxime Parent:** Software, Formal analysis, Writing - Review & Editing, Visualization. **Fahmeed Hyder:** Methodology, Resources, Writing - Review & Editing, Project administration, Funding acquisition. **Kenneth Roberts:** Methodology, Writing - Review & Editing. **Ravinder Nath:** Resources. **Olivier Tillement:** Methodology, Resources, Writing - Review & Editing. **Donald Engelman:** Methodology, Resources, Writing - Review & Editing, Supervision, Funding

acquisition; **Peter Glazer:** Methodology, Resources, Writing - Review & Editing, Supervision, Funding acquisition.

References

[1] J. Schuemann, R. Berbeco, D.B. Chithrani, S.H. Cho, R. Kumar, S.J. McMahon, S. Sridhar, S. Krishnan, Roadmap to clinical use of gold nanoparticles for radiation sensitization, Int. J. Radiat. Oncol. Biol. Phys. 94 (2016) 189–205.

[2] F. Lux, V.L. Tran, E. Thomas, S. Dufort, F. Rossetti, M. Martini, C. Truillet, T. Doussineau, G. Bort, F. Denat, F. Boschetti, G. Angelovski, A. Detappe, Y. Cremillieux, N. Mignet, B.T. Doan, B. Larrat, S. Meriaux, E. Barbier, S. Roux, P. Fries, A. Muller, M.C. Abadjian, C. Anderson, E. Canet-Soulas, P. Bouziotis, M. Barberi-Heyob, C. Frochot, C. Verry, J. Balosso, M. Evans, J. Sidi-Boumedine, M. Janier, K. Butterworth, S. McMahon, K. Prise, M.T. Aloy, D. Ardail, C. Rodriguez-Lafrasse, E. Porcel, S. Lacombe, R. Berbeco, A. Allouch, J.L. Perfettini, C. Chargari, E. Deutsch, G. Le Duc, O. Tillement, AGuIX((R)) from bench to bedside-Transfer of an ultrasmall theranostic gadolinium-based nanoparticle to clinical medicine, The British Journal of Radiology 91 (2018) 1–19 20180365.

[3] H. Maeda, H. Nakamura, J. Fang, The EPR effect for macromolecular drug delivery to solid tumors: Improvement of tumor uptake, lowering of systemic toxicity, and distinct tumor imaging in vivo, Adv. Drug Deliv. Rev. 65 (2013) 71–79.

[4] J.F. Hainfeld, D.N. Slatkin, H.M. Smilowitz, The use of gold nanoparticles to enhance radiotherapy in mice, Phys. Med. Biol. 49 (2004) N309–N315.

[5] D.B. Chithrani, M. Dunne, J. Stewart, C. Allen, D.A. Jaffray, Cellular uptake and transport of gold nanoparticles incorporated in a liposomal carrier, Nanomed. Nanotechnol. Biol. Med. 6 (2010) 161–169.

[6] S. Kotb, A. Detappe, F. Lux, F. Appaix, E.L. Barbier, V.L. Tran, M. Plissonneau, H. Gehan, F. Lefranc, C. Rodriguez-Lafrasse, C. Verry, R. Berbeco, O. Tillement, L. Sancey, Gadolinium-based nanoparticles and radiation therapy for multiple brain melanoma metastases: proof of concept before phase I trial, Theranostics 6 (2016) 418–427.

[7] E. Lechtman, N. Chattopadhyay, Z. Cai, S. Mashouf, R. Reilly, J.P. Pignol, Implications on clinical scenario of gold nanoparticle radiosensitization in regards to photon energy, nanoparticle size, concentration and location, Phys. Med. Biol. 56 (2011) 4631–4647.

[8] K. Huang, H. Ma, J. Liu, S. Huo, A. Kumar, T. Wei, X. Zhang, S. Jin, Y. Gan, P.C. Wang, S. He, X. Zhang, X.J. Liang, Size-dependent localization and penetration of ultrasmall gold nanoparticles in cancer cells, multicellular spheroids, and tumors in vivo, ACS Nano 6 (2012) 4483–4493.

[9] L. Sancey, F. Lux, S. Kotb, S. Roux, S. Dufort, A. Bianchi, Y. Cremillieux, P. Fries, J.L. Coll, C. Rodriguez-Lafrasse, M. Janier, M. Dutreix, M. Barberi-Heyob, F. Boschetti, F. Denat, C. Louis, E. Porcel, S. Lacombe, G. Le Duc, E. Deutsch, J.L. Perfettini, A. Detappe, C. Verry, R. Berbeco, K.T. Butterworth, S.J. McMahon, K.M. Prise, P. Perriat, O. Tillement, The use of theranostic gadolinium-based nanoprobes to improve radiotherapy efficacy, Br. J. Radiol. 87 (2014) 20140134.

[10] R. Liu, T. Zhao, X. Zhao, F.J. Reynoso, Modeling gold nanoparticle radiosensitization using a clustering algorithm to quantitate DNA double-strand breaks with mixed-physics Monte Carlo simulation, Med. Phys. 46 (2019) 5314–5325.

[11] A. Detappe, S. Kunjachan, J. Rottmann, J. Robar, P. Tsiamas, H. Korideck, O. Tillement, R. Berbeco, AGuIX nanoparticles as a promising platform for image-guided radiation therapy, Cancer Nanotechnol 6 (2015) 4.

[12] A.A. Svoronos, R. Bahal, M.C. Pereira, F.N. Barrera, J.C. Deacon, M. Bosenberg, D. DiMaio, P.M. Glazer, D.M. Engelman, Tumor-Targeted, Cytoplasmic Delivery of Large, Polar Molecules using a pH-Low Insertion Peptide, Mol Pharm, 2019.

[13] N. Chattopadhyay, Z. Cai, Y.L. Kwon, E. Lechtman, J.P. Pignol, R.M. Reilly, Molecularly targeted gold nanoparticles enhance the radiation response of breast cancer cells and tumor xenografts to X-radiation, Breast Cancer Res. Treat. 137 (2013) 81–91.

[14] J.F. Hainfeld, M.J. O'Connor, F.A. Dilmanian, D.N. Slatkin, D.J. Adams, H.M. Smilowitz, Micro-CT enables microlocalisation and quantification of Her2-targeted gold nanoparticles within tumour regions, Br. J. Radiol. 84 (2011) 526–533.

[15] J.C. Deacon, D.M. Engelman, F.N. Barrera, Targeting acidity in diseased tissues: mechanism and applications of the membrane-inserting peptide, pHLIP, Arch. Biochem. Biophys. 565 (2015) 40–48.

[16] M. Anderson, A. Moshnikova, D.M. Engelman, Y.K. Reshetnyak, O.A. Andreev, Probe for the measurement of cell surface pH in vivo and ex vivo, Proc. Natl. Acad. Sci. U. S. A. 113 (2016) 8177–8181.

[17] Y.K. Reshetnyak, L. Yao, S. Zheng, S. Kuznetsov, D.M. Engelman, O.A. Andreev, Measuring tumor aggressiveness and targeting metastatic lesions with fluorescent pHLIP, Mol. Imaging Biol. 13 (2011) 1146–1156.

[18] E. Thomas, L. Colombeau, M. Gries, T. Peterlini, C. Mathieu, N. Thomas, C. Boura, C. Frochot, R. Vanderesse, F. Lux, M. Barberi-Heyob, O. Tillement, Ultrasmall AGuIX theranostic nanoparticles for vascular-targeted interstitial photodynamic therapy of glioblastoma, Int. J. Nanomedicine 12 (2017) 7075–7088.

[19] D. Kryza, J. Taleb, M. Janier, L. Marmuse, I. Miladi, P. Bonazza, C. Louis, P. Perriat, S. Roux, O. Tillement, C. Billotey, Biodistribution study of nanometric hybrid gadolinium oxide particles as a multimodal SPECT/MR/optical imaging and theragnostic agent, Bioconjug. Chem. 22 (2011) 1145–1152.

[20] S. Kotb, J. Piraquive, F. Lamberton, F. Lux, M. Verset, V. Di Cataldo, H. Contamin, O. Tillement, E. Canet-Soulas, L. Sancey, Safety evaluation and imaging properties of gadolinium-based nanoparticles in nonhuman primates, Sci. Rep. 6 (2016) 35053.

[21] Y.K. Reshetnyak, O.A. Andreev, U. Lehnert, D.M. Engelman, Translocation of molecules into cells by pH-dependent insertion of a transmembrane helix, Proc. Natl. Acad. Sci. U. S. A. 103 (2006) 6460–6465.

[22] W. Rima, L. Sancey, M.T. Aloy, E. Armandy, G.B. Alcantara, T. Epicier, A. Malchere, L. Joly-Pottuz, P. Mowat, F. Lux, O. Tillement, B. Burdin, A. Rivoire, C. Boule, I. Anselme-Bertrand, J. Pourchez, M. Cottier, S. Roux, C. Rodriguez-Lafrasse, P. Perriat, Internalization pathways into cancer cells of gadolinium-based radiosensitizing nanoparticles, Biomaterials 34 (2013) 181–195.

[23] M.H. Spitzer, G.P. Nolan, Mass cytometry: single cells, many features, Cell 165 (2016) 780–791.

[24] D. Coman, Y. Huang, J.U. Rao, H.M. De Feyter, D.L. Rothman, C. Juchem, F. Hyder, Imaging the intratumoral-peritumoral extracellular pH gradient of gliomas, NMR Biomed. 29 (2016) 309–319.

[25] R.D. Jiang, H. Shen, Y.J. Piao, The morphometrical analysis on the ultrastructure of A549 cells, Romanian J. Morphol. Embryol. 51 (2010) 663–667.

[26] M. Luchette, H. Korideck, M. Makrigiorgos, O. Tillement, R. Berbeco, Radiation dose enhancement of gadolinium-based AGuIX nanoparticles on HeLa cells, Nanomed. Nanotechnol. Biol. Med. 10 (2014) 1751–1755.

[27] X. Zhang, Y. Lin, R.J. Gillies, Tumor pH and its measurement, J. Nucl. Med. 51 (2010) 1167–1170.

[28] Y. Huang, D. Coman, P. Herman, J.U. Rao, S. Maritim, F. Hyder, Towards longitudinal mapping of extracellular pH in gliomas, NMR Biomed. 29 (2016) 1364–1372.

[29] D.B. Leeper, K. Engin, J.H. Wang, J.R. Cater, D.J. Li, Effect of i.v. glucose versus combined i.v. plus oral glucose on human tumour extracellular pH for potential sensitization to thermoradiotherapy, Int. J. Hyperth. 14 (1998) 257–269.

[30] J. Naeslund, K.E. Swenson, Investigations on the pH of malignant tumors in mice and humans after the administration of glucose, Acta Obstet. Gynecol. Scand. 32 (1953) 359–367.

[31] D. Weerakkody, A. Moshnikova, M.S. Thakur, V. Moshnikova, J. Daniels, D.M. Engelman, O.A. Andreev, Y.K. Reshetnyak, Family of pH (low) insertion peptides for tumor targeting, Proc. Natl. Acad. Sci. U. S. A. 110 (2013) 5834–5839.